JOURNAL OF OPTOELECTRONICS LASER ISSN: 1005-0086

Volume 41 Issue 8, 2022

# Detection of Gliomas in Spinal Cord Using U-Net++ Segmentation with Xg_Boost Classification

**Para Rajesh[*1], A. Punitha[2] & P. Chandra Sekhar Reddy[3]**

*[*1&3]Computer Science and Engineering Dept, Gokaraju Rangaraju Institute of Engineering and Technology Hyderabad-500090, Telangana, India*

*[2]Computer Science and Engineering Dept, Annamalai University, Annamalai Nagar - 608002, Tamil Nadu, India*

**ABSTRACT**

Gliomas are the most common primary brain tumors. They are classified into 4 grades (Grade I–II-III–IV) according to the guidelines of the World Health Organization (WHO). The accurate grading of gliomas has clinical significance for planning prognostic treatments, pre-diagnosis, monitoring and administration of chemotherapy. This paper propose the novel technique in early detection of Gliomas in spinal cord based on segmentation and classification techniques by deep learning architectures. Here the input image has been pre-processed for noise removal, image resizing and smoothening of the image. Then this processed image has been segmented using U-Net++ architecture in which the skull or vertebral column parts has been segmented and classified using XG_Boost architecture. The performance of our method on a publicly available MRI image dataset of 3064 slices from 233 patients is compared with previously classical machine learning and deep learning published methods. In the comparison, our method remarkably obtained a tumor classification accuracy of 0.965, higher than the other approaches using the same database.

**Keywords:** Gliomas, brain tumors, segmentation, classification, deep learning.

## I. INTRODUCTION

Gliomas are primary malignant tumors that are common in the brain, having a high relapse rate and high mortality. According to the data of the American Cancer Society, 23,880 people were diagnosed with malignant brain and spinal cord tumors in 2018 and 70% of those diagnosed with malignant tumors died [1]. Gliomas are usually classified in a range of grades from I to IV. According to the classification of the World Health Organization (WHO), gliomas can be subdivided by their malignancy from Grade II (lower grade) to Grade IV (high grade) [2]. Gliomas, hypoyphosis tumors and meningiomas are among the primary brain tumors [3]. The WHO categorization includes low-grade gliomas (LGGs), diffuse low-grade (Grade II) and medium-grade gliomas (Grade III), and tumors with highly variable behaviors whose textural structures are unpredictable. In addition, according to the WHO, low-grade gliomas are infiltrative neoplasms that usually contain low and medium-grade gliomas (Grade II and Grade III) [4]. Grade II and Grade III brain tumors can have types of astrocytoma, oligoastrocytoma, oligodendrioglioma. These tumors can be in Grade II and Grade III groups, therefore, examining brain tumor types in the right classes will facilitate the treatment of brain cancers. Astrocytomas can be low grade (Grade II) and high grade (Grade III). Low grade astrocytomas grow slowly in a certain area. High-grade astrocytomas grow rapidly and require different treatment methods [5]. The tissues of Grade II tumors are malignant and these cells do not look very much like normal cells. Grade III tumors are malignant tissue cells and these cells also grow actively. Classifying Grade II and Grade III tumors, both cellular and MRI images, is quite complex and clinically demanding. Automatic segmentation and classification of medical images play an important role in diagnostics, growth prediction, and treatment of brain tumors. An early tumor brain diagnosis implies a faster response in treatment, which helps to improve patients' survival rate. Location and classification of brain tumors in large medical images databases, taken in routine clinical tasks by manual procedures, have a high cost both in effort and time. An automatic detection, location, and classification procedure is desirable and worthwhile. There are several medical imaging techniques used to acquire information about tumors (tumor type, shape, size, location, etc.), which are needed for their diagnosis [5]. The most important techniques are Computed Tomography (CT), Single-Photon-Emission Computed Tomography (SPECT), Positron Emission Tomography (PET), Magnetic Resonance Spectroscopy (MRS), and Magnetic Resonance Imaging (MRI). These techniques can be combined to obtain more detailed information about tumors. Anyhow, MRI is the most used technique due to its advantageous characteristics. In MRI acquisition, the scan provides hundreds of 2D image slices with high soft tissue contrast using no ionizing radiation. There are four MRI modalities used in diagnosis: T1-weighted MRI (T1), T2-weighted MRI (T2), T1-weighted contrast-enhanced MRI (T1-CE), and Fluid Attenuated Inversion Recovery (FLAIR). Each MRI modality produces images with different tissue contrasts; thus, some are more suited to search a specific kind of tissue than others. T1 modality is typically used to work with healthy tissues[6].

The rest of the paper is sorted out as follows: Section 2 exhibits about literature review on crops. Section 3 presents a proposed gliomas detection design. Section 4 depicts the experimental results. Section 5 concludes the paper with future scope.

## II. RELATED WORKS

Recently, Machine learning (ML) and Deep Learning (DL) methods are widely been used for detection and grading brain tumors using different imaging modalities, especially those acquired using MRI. In this section, the most recent and related research works on the paper topic are presented. Work [7] proposes a system that combines discrete wavelet transform (DWT) features and

deep learning (DL) techniques. They have used fuzzy c-mean method for segmenting the brain tumor, and for each detected lesion the DWT was applied to extract the features, where these features are fed into the principal component analysis (PCA) for feature dimension reduction and finally the selected features are then fed to deep neural networks (DNN). The results show that they achieve an accuracy rate of 96.97% and a sensitivity of 97.0 %. Research in [8] presented a brain tumor classification system using a convolutional neural network (CNN) and Gray Level Co-occurrence Matrix (GLCM) based features. They extracted four features (Energy, Correlation, Contrast, and Homogeneity) from four angles (0°, 45°, 90°, and 135°) for each image and then these features are fed into CNN, they tested their methodology on four different datasets (Mg-Gl, Mg-Pt, Gl-Pt, and Mg-Gl-Pt) and the best accuracy achieved was82.27% for Gl-Pt dataset using two sets of features; contrast with homogeneity and contrast with correlation. Author [9] proposed a deep CNN based system for automated brain tumor detection and grading. The system is based on Fuzzy C-Means (FCM) for brain segmentation and based on these segmented regions a texture and shape features were extracted then these features were fed into SVM and DNN classifiers. The results showed that the system achieved a rate of 97.5% accuracy. On the other hand, work [10] enhanced the performance of the brain tumor classification process using region of interest (ROI) augmentation and fine ring-form partition. They applied these enhancements to different feature extractions methods which are intensity histogram, GLCM, and the bag-of-words (BoW) where these features vectors are fed into a classifier. The experimental results showed that the accuracy enhanced from 71.39% to 78.18%, and 83.54% to 87.54%, and 89.72% to 91.28% for intensity histogram, GLCM, and BoW respectively. Author [11] proposed a genetic algorithm feature selection for feature dimension reduction of wavelet features set. The method is based on selecting optimal features vector that can be fed into the selected classifier such as an artificial neural network (ANN). The results show that the genetic algorithm selected only 4 of 29 features and achieved an accuracy of 98% using only the selected features. in [12] author proposed a system for non-invasive grading of glioma brain tumors using a modified version of AlexNet CNN. The classification process was done using whole-brain MRI images and the labels of the images were at the image level, not the pixel level. The experimental results showed that the method achieved a reasonable performance with an accuracy of 91.16%. work [13] proposed an extensive data augmentation method fused with CNN for brain tumor classification. The method used for multi-grade classification of brain tumors using segmented brain tumor MRI images. They used pretrained VGG-19 CNN architecture for classification using transferee learning and achieved an overall accuracy of values 87.38% and 90.67% for data before and after augmentation respectively. While work in [14] combine the CNN with neutrosophic expert maximum fuzzy (NS-CNN) sure entropy for brain tumor classification. They used the neutrosophic set – expert maximum fuzzy-sure method for brain tumor segmentation then these images are fed to CNN to extract features and fed them to SVM classifiers to be classified as benign or malignant. They achieved an average success of 95.62%.author [15] developed a novel cuckoo search with a crossover algorithm that could accurately classify a variety of cancer subtypes. The model was tested on benchmark cancer gene expression, and the results show that CSC outperformed CS and other well-known methods. Work in [16] used the relief algorithm for dimension reduction and feature ranking. The most important features were then used by support vector machines (SVM) and convolutional neural networks (CNN) [17] for prediction. The experimental results show that the proposed approach could improve the accuracy of SVM and CNN classification methods. Finally, author [18] suggested a novel multivariate feature ranking approach to increase gene selection efficiency in microarray data.

## III. MATERIALS AND METHODS

In this paper, we applied a U-Net++ architecture network for tumor segmentation and XG_Boost architecture based classification. We initially used a single U-Net++ and sent all training dataset to that network for segmentation and classification. All dataset images are grayscale and the foreground of the images are located at the center. Images are captured from different views of the skull; hence the size and position of the tumors vary in different angles. These differences in the size of the tumors make the diagnosis of the tumor hard. In practice, the expert physician knows the direction that the MR image is captured. Since the learning process in deep networks is similar to the human learning process, we decided to create the same situation for the deep neural networks. We found out using a single network for identification of tumors in all images does not produce accurate results. The overall proposed architecture is shown in figure-1.

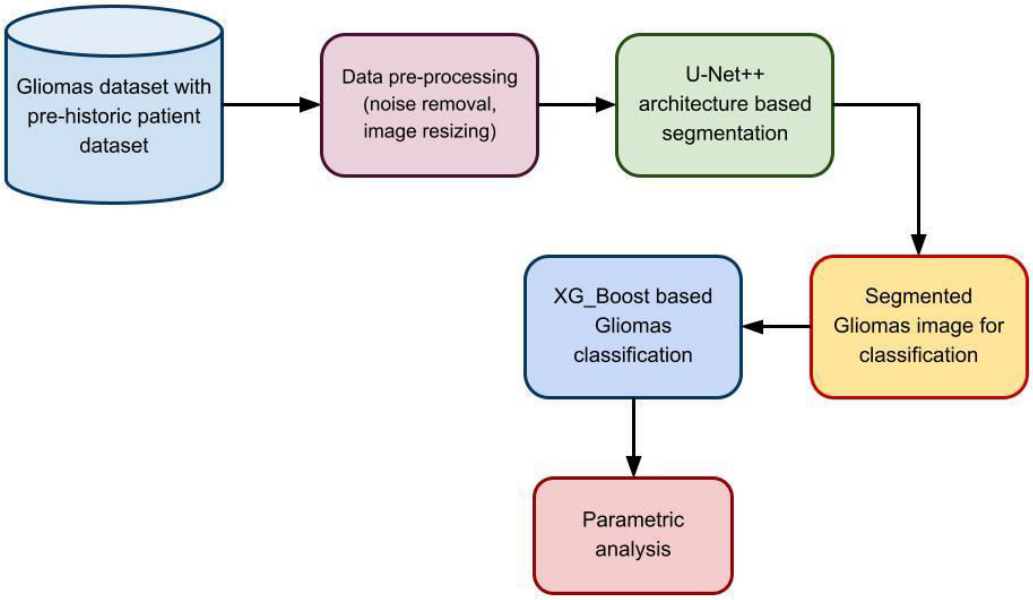


**Figure-1 Overall Proposed architecture**

**Dataset description and Data Pre-processing**

In clinical settings, usually only a certain number of slices of brain CE-MRI with a large slice gap, not a 3D volume, are acquired and available. It is difficult to build a 3D model with such sparse data. Hence, the proposed method is based on 2D slices collected from 233 patients, acquired from Nanfang Hospital, Guangzhou, China, and General Hospital, Tianjing Medical University, China, from 2005 to 2010. This dataset contains 3064 slices and includes meningiomas (708 slices), gliomas (1426 slices), and pituitary tumors (930 slices) in the common views (sagittal, coronal, and axial). Figure 1 shows examples of these three types of tumors. This dataset provides also 5-fold cross-validation indices. By using this information, 80% (2452) of the images are employed for training and 20% (612 images) are used for obtaining performance measurements. The process is repeated 5 times. The images have an in-plane resolution of 512 × 512 pixels with pixel size 0.49 × 0.49 mm2 . The slice thickness is 6 mm, and the slice gap is 1 mm. The tumor border was manually delineated by three experienced radiologists. Every slice in the dataset has an information structure attached containing the patient's pid; the tumor type label (lgt ): 1 for meningioma, 2 for glioma, and 3 for pituitary tumor; the coordinates vector (x,y) of the points belonging to the tumor border, and the tumor mask (Tij): a binary image where the tumor positions contain a value of 1 and the healthy ones a value of 0. The pair lgt ,Tij will be the ground truth in the training process. During training, data augmentation using an elastic transform has been used to prevent overfitting of the neural network. Data augmentation procedure doubled the number of training images available on each fold iteration up to 4904 images. A thorough process was conducted to extract 65 × 65 px training examples from every image in the training dataset: 150 true positive window examples and 325 true negative window examples per tumor. The pixels on these windows were scaled using pixel standardization (zero mean and unit variance) across the entire training dataset.

**U-Net++ based Gliomas segmentation:**

In previous baseline architecture, no contextual information is shared between the shallow and deep layers. There is a need to introduce a module which can create an information bridge between shallow and deep layers so that local and global features of the network can be enhanced. Figure 2 shows the overall architecture of the proposed BU-Net, which includes RES blocks and a WC block. The architecture takes input images of resolution 256 × 256 and outputs the images with the same dimensions. The left part of the model act as an encoder and the right part of the model acts as a decoder. The convolution layers with padding are used in U-Net++. This allows getting the same sized image as the output as that given as input. The encoder and decoder of the network are divided into blocks. On the encoder side every block consists of two convolution layers along with a single max-pooling layer and a dropout layer. Every block of the decoder side starts with the Conv2DTranspose layer applied on the output of the previous block. The output of Conv2DTranspose layer is concatenated with the output generated from the associated RES block. Dropout is applied to the concatenated output followed by two convolution layers. The last block of the decoder includes another convolution layer with six filters of size 1 × 1. The encoder side performs the contraction process on the image, and the decoder side performs the expansion process.

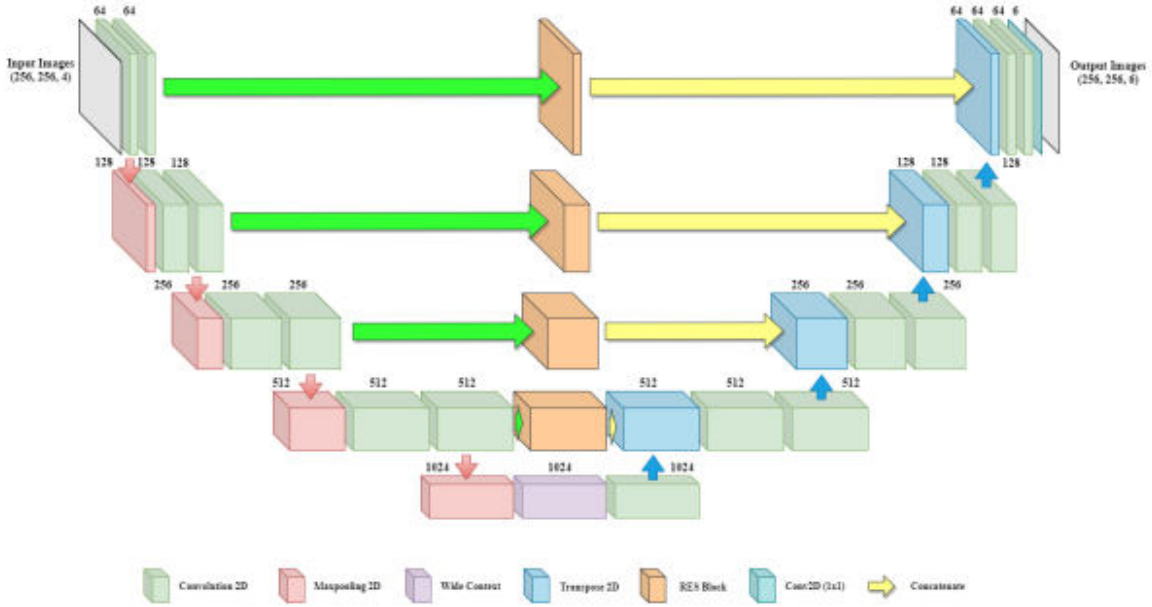

**Figure-2 Proposed U-Net++ architecture in Gliomas segmentation**

Further, for the transition from the encoder to the decoder, the architecture uses a wide context block. All the convolution layers of U-Net++are followed by batch normalization and ReLU activation function, except for the last convolution layer, which uses a sigmoid activation function. The numerical representations of ReLU and sigmoid activation function are as follows:

$$\mathrm{ReLU}(q) = \begin{cases} 0, & \text{if } q \leq 0 \\ q, & \text{otherwise} \end{cases}$$

$$\mathrm{Sigmoid}(q) = \frac{1}{1 + \exp(-q)}$$

The U-Net++ is implemented on Keras framework [37]. To set the dropout ratio, we applied hyper-parameter tuning—a range of dropout ratios were tested to get the most optimal dropout ratio; 0.3 proved to be the most optimal dropout ratio for the network. Adam optimizer was used along with the customized loss function. The learning rate was set to 0.01 with a momentum of 0.9. The batch size was 16, and early stopping based on validation loss with patience level of 10 was utilized for the maximum number of training iterations.

The input to the architecture is given to 5 parallel connections. In the first four of them, two convolutions layers are applied. In each connection with convolution layers, we have used N × 1 filter size for first convolution layer and 1 × N filter size for second convolution layer. We used two cascaded convolution layers rather than using a single convolution layer with the filter size of N × N. Using two convolution layers generates a lesser number of parameters which benefits the overall architecture. Moreover, during experiments, the observation was made that the impact of cascaded convolution layers with the lower number of parameters is similar to that of a single layer of convolution having a higher number of parameters. The last connection is a skip connection where the input is as it is forwarded. All the outputs from five connections are summed up to get a single output. Three convolution layers one after another are applied on the summed output. The three convolution layers have filter sizes of 3 × 3, 3 × 3, and 1 × 1. The RES block generates the middle-level features from the low-level features, which helps to control the information degradation. The cancer regions have high size variations for which residual extended skip performs contextual aggregation on multiple scales, which makes it scale-invariant. The RES increases the valid receptive field, and this allows the U-Net++ to have better segmentation.

The input to WC is given to two parallel connections. Both the connections have 2 convolution layers. In the first connection, the two convolution layers use N × 1 and 1 × N respectively. The second connection first uses the 1 × N filter size, and then the next convolution layer has filter size N × 1. This change in combination in both the connections makes up a good feature set which can contribute towards the performance. The observation was made that a change in combination changes the extracted features, and both the combinations can contribute towards the final result. The outputs from both connections are summed up and treated as an output of WC. The wide context (WC), similarly to RES, extracts the contextual information which is important for sub-classification between different sub-classes of cancer. Further, it performs the feature aggregation at the transition level, which leads to a better reconstruction of the segmented regions.

The total area covered by healthy tissues in brain tumor MRI is 98.46%. The edema region covers 1.02% and the enhancing tumor region covers 0.29% of brain tumor MRI image. The lowest volume is covered by the non-enhancing tumor, which is only 0.23%. The large difference has a severe effect on the segmentation performance. The loss function is composed of two objective functions: one objective function is used to get maximum overlap between the ground truth and predicted segmented regions regardless of the class, which is performed by Dice loss coefficient (DLC); and the second objective function is responsible for classifying the tissue cells concerning their class, which is performed by weight cross-entropy (WCE).

**XG-Boost based Gliomas Classification**

XGBoost is an efficient gradient-boosted decision tree algorithm. Gradient boosting is a technique introduced by XGB. The new models are fitted to residuals from previous models, and the combined results are minimized using gradient descent. Classification of tumors can be performed using a number of factors, and depending upon the type of data large number of features can be extracted, using which an efficient medical diagnostic system can be realized. We could classify tumors and brain images as normal, abnormal and neutral ones or we could decide whether the tumor is benign or malignant. Our work focuses on the latter part and results are obtained on a dataset of over fifty images. The usage of learning models, both supervised and unsupervised are being used widely to come up with the most efficient classifier and improvements as well as hybrid approaches are being tried and tested for the same. Random forests and decision trees offer an interesting perspective and Extreme Gradient Boosted Decision Trees have been recently shown to be an accurate alternative compared to all the other learning models. We implement it using the extreme gradient boost library XGBoost. Extreme Gradient Boosted Machines (EGBM) are a supervised learning model that take weak learners or classifiers and collate them to form a strong classifier. Weak learners have high biases and low variances as opposed to Random Forests (RF) which use learners with low biases but high variance. They are better than neural nets because we have the ability to see how and why a computer takes a decision. Suppose we have two weak learners or two classifier trees that each show some property of the problem, are different but weak as separate entities. In RF, we keep building the trees in parallel, but in XGBoost we instead move in iterative steps, where weak classifiers are used to build upon one another so that at each step we have the most optimal step. Instead of working separately each weak learner now builds upon the previous tree and hence we optimize each step. So if we have one tree with two conditions (C1, C2) (Fig. 8. (a)) and the other tree with condition C3, then if the value for the entity A has to be found, boosted value is the sum of both weak learners, A=2+.5, and so on. We prune the final tree in a bottom-up parsing and since the entire tree has been made the user is aware of the depth as well. These ensemble tree methods with iterative improvements and sequential structure has shown more accurate and quicker results than traditional GBMs and is done by verifying through 5-fold cross-validation [14, 15]. Our usage showed 100% accurate results for brain tumor classification using 50 images and cross-validating for the results. The results were as we expected and computation was performed in extremely low times.

The idea is to continuously add tree and continuously perform feature splitting to grow a tree.

$$\hat{y}_i = \phi(x_i) = \sum_{k=1}^{T} f_k(x_i), f_k \in \mathcal{F}$$

Defining the function as follows.

$$\mathcal{F} = \{f(x) = w_{q(x)}\}(q: R^m \to T, w \in R^T)$$

in which y^iy^i is the predicted label of *i*th sample, $x_i$ represents the *i*th sample, *T* represents the total number of trees, $f_k$ represents the *kth* tree model, and *q* represents the structure of each tree that maps an example to the corresponding leaf index. The objective function of XGBoost classifier is defined as

$$L(\phi) = \sum_{i=1}^{n} l(\hat{y}_i, y_i) + \sum_{k=1} \Omega(f_k), \text{ where } \Omega(f) = \gamma T + \frac{1}{2}\lambda \parallel w \parallel^2$$

There are two terms in the objective function. The first term is the loss function measuring the difference between the predicted value and the real value. The second term is the regularization term. *T* and *w* refer to the number of leaf nodes and the weight of leaf nodes, respectively. γ controls the number of leaf nodes, and λ is used to prevent overfitting. Each time when a tree is added, it automatically learns a new function to fit the residuals arising from the last prediction. If we obtain *k* trees after training, it is necessary to sum the scores corresponding to each tree to get the predicted value of a sample. In the research, we choose XGBoost classifier, the maximum depth of which is nine, learning rate γ is 0.1, and λ is 0.3 by 10-fold cross-validation as the model for numerical experiments.

## IV. EXPERIMENTAL ANALYSIS

In this section, we present the findings of the various experiments to judge the performance of the proposed hybrid model. A PC with the following features was used to test the proposed hybrid model: Intel(R) Core (TM) i5-7500 CPU with a 32-bit operating system, 4 GB RAM, and the Windows 7 operating system as well as the NumPy, SciPy, Pandas, Keras, and Matplotlib frameworks and Python 2.7 programming language.

Molecular profiles from 28 patient samples were analyzed (data set A: medulloblastomas, CNS AT/RTs, renal and extrarenalrhabdoid tumors, supratentorial PNETs, and normal human cerebella). In our experiments, we used eight-fold cross-validation to evaluate the outcomes of the proposed hybrid model, and the results are represented as an average standard

deviation. Furthermore, the total number of iterations in all of the experiments was 30. In our experiments, we used three evaluation methods: Accuracy, Precision, recall, F-1 Score.

The stated parameters are evaluated with the estimation of True Positive (TP), False Negative (FN), True Negative (TN), and False Positive (FP).

***Accuracy:*** It defined the number of correctly predicted values to the total number of predictions. It is defined as

$$\text{Accuracy} = \frac{TP+TN}{TP+TN+FP+FN}$$

***Recall or Sensitivity:*** It is defined as the correctly predicted value to the total prediction value. It is defined as

$$\text{Recall} = \frac{TP}{TP+FN}$$

***Precision***: It provides the ratio of true positive values to the total predicted values. It is stated as

$$\text{Precision} = \frac{TP}{TP+FP}$$

***F1 - Score:*** It provides the ratio between average mean of precision and recall. F1-Score is stated as

$$F1 - Score = 2^{*}\frac{\text{Precision} * \text{Recall}}{\text{Precision} + \text{Re call}}$$

**Table-1 Comparative analysis between proposed and existing technique**

| Parameters (%) | CNN | KNN | SVM | DNN | U-net_VGG-19 | U-net++_XGboost (propose) |
|---|---|---|---|---|---|---|
| **Accuracy** | 88 | 89 | 91 | 93 | 93.51 | 96.9 |
| **Precision** | 86 | 85 | 84 | 94.1 | 93.3 | 96.97 |
| **Recall** | 77 | 75 | 76 | 87.5 | 92.43 | 96.27 |
| **F1 - Score** | 79 | 80 | 81 | 80 | 92 | 96.56 |

The above table-1 shows comparative analysis between proposed and existing technique in Gliomas detection based on segmentation and classification techniques. Here the proposed technique has been compared with CNN,KNN,SVM, DNN and U-net_VGG-19. The comparative graphs has been shown below.

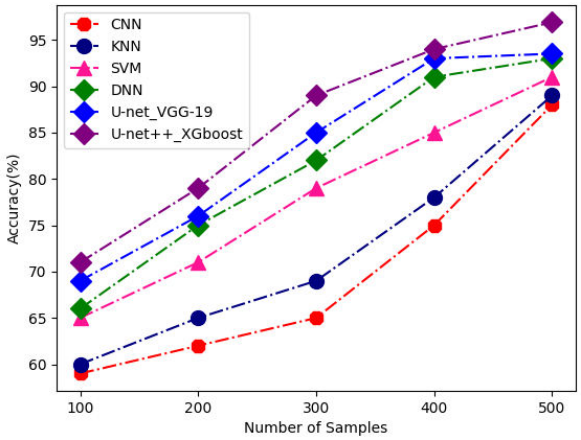


**Figure-3 Comparative analysis of Accuracy**

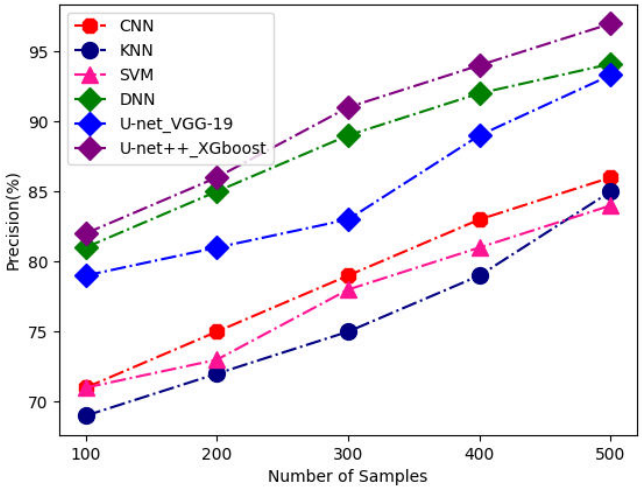

**Figure-4 Comparative analysis of Precision**

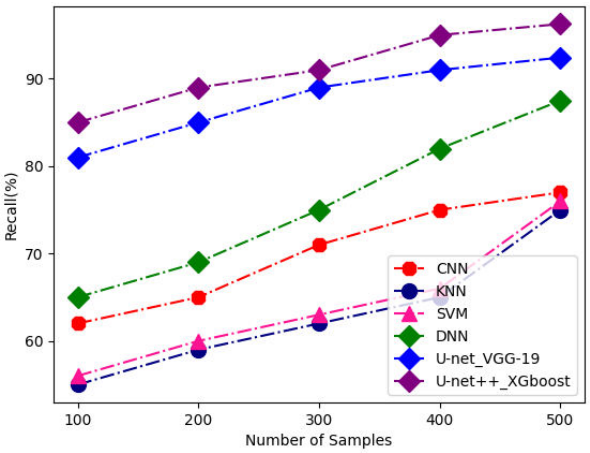


**Figure-5 Comparative analysis of Recall**

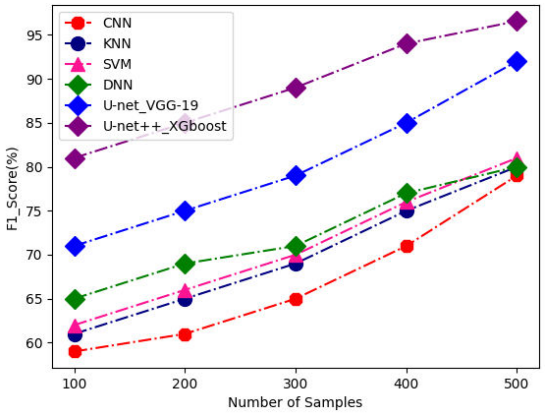


**Figure-5 Comparative analysis of F-1 score**

The above figure 2-5 shows the comparative analysis based on proposed and existing techniques in Gliomas detection. Here the proposed technique obtained optimal results in terms of accuracy, precision, recall and F-1 score. The proposed technique U-net++_XGboost obtained accuracy of 96.9%, precision of 96.97%, recall of 96.27% and F-1 score of 96.56%.when compared with existing the accuracy in detecting the tumor is enhanced with minimal computational time. The overall comparison is shown in figure-6.

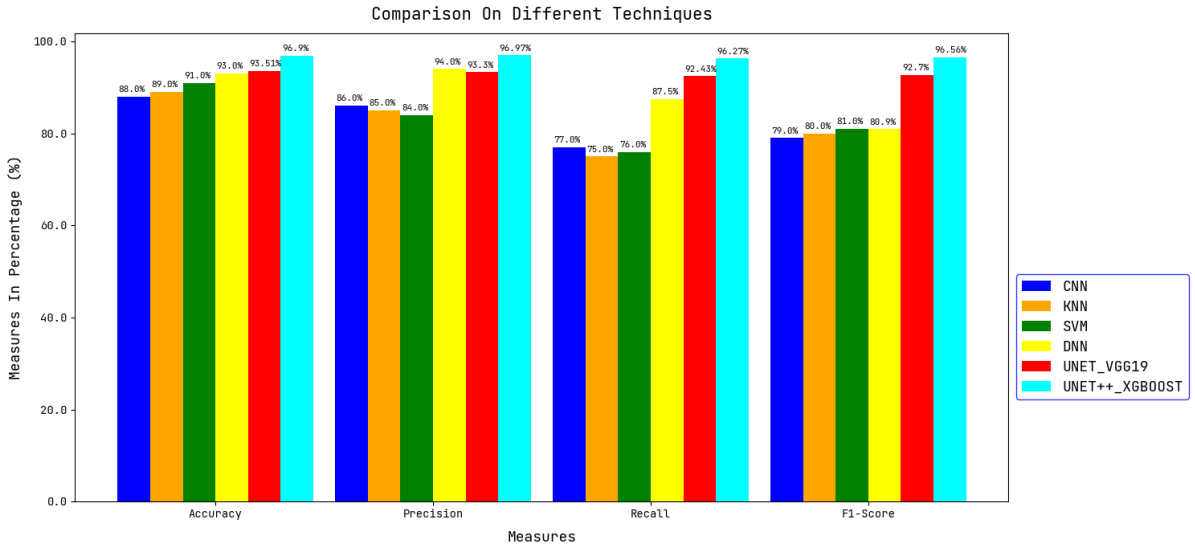


**Figure-6 Overall parametric comparison in Gliomas detection**

## V. CONCLUSION

This paper proposed novel technique in early detection of Gliomas using deep learning based segmentation and classification. Here We evaluated its performance using a publicly available T1-weighted contrast-enhanced MRI images dataset. Data augmentation through elastic transformation was adopted to increase the training dataset and prevent overfitting. For the definite segmentation of brain tumors, we have proposed a novel model with modifications in encoder–decoder architecture. We have introduced two new blocks, namely, residual extended skip (RES) and wide context (WC), into the U-Net++ architecture. Then XG_Boost based classifier is used and adds regular terms to the cost function for controlling the complexity of the model, which contains the number of leaf nodes in the tree and the score sum of squares on each leaf node. From the perspective of bias variance, the regular term reduces the variance of the classifier and simplifies the learned classifier. so it can better prevent overfitting in training and its performance is the best compared to the other four classifiers. The results may provide a useful revelation to determine the machine learning model and to understand actual pathological conditions. The measures of performance obtained are in the range of the top ten methods from the BRATS 2013 benchmark. We compared our results with other seven brain tumor classification approaches that used the same dataset. Our method obtained the highest tumor classification accuracy with a value of 0.965.

## REFERENCES

[1] Siegel, R.L.; Miller, K.D.; Jemal, A. Cancer statistics, 2021. CA A Cancer J. Clin. 2021, 66, 7–30.
[2] Rehman, M.U.; Cho, S.; Kim, J.; Chong, K.T. BrainSeg-Net: Brain Tumor MR Image Segmentation via Enhanced Encoder–Decoder Network. Diagnostics 2021, 11, 169.
[3] Isensee, F.; Jäger, P.F.; Full, P.M.; Vollmuth, P.; Maier-Hein, K.H. nnU-net for brain tumor segmentation. In International MICCAI Brainlesion Workshop; Springer: Cham, Switzerland, 2020; pp. 118–132.
[4] Zeineldin, R.A.; Karar, M.E.; Coburger, J.; Wirtz, C.R.; Burgert, O. DeepSeg: Deep neural network framework for automatic brain tumor segmentation using magnetic resonance FLAIR images. Int. J. Comput. Assist. Radiol. Surg. 2020, 15, 909–920
[5] Perrin, S.L.; Samuel, M.S.; Koszyca, B.; Brown, M.P.; Ebert, L.M.; Oksdath, M.; Gomez, G.A. Glioblastoma heterogeneity and the tumour microenvironment: Implications for preclinical research and development of new treatments. Biochem. Soc. Trans. 2019, 47, 625–638.
[6] Rehman, M.U.; Cho, S.; Kim, J.H.; Chong, K.T. BU-Net: Brain Tumor Segmentation Using Modified U-Net Architecture. Electronics 2020, 9, 2203.
[7] Pei, L.; Vidyaratne, L.; Rahman, M.; Iftekharuddin, K.M. Context aware deep learning for brain tumor segmentation, subtype classification, and survival prediction using radiology images. Sci. Rep. 2020, 10, 1–11.
[8] Pradana, A.C.; Aditsania, A. Implementing binary particle swarm optimization and C4.5 decision tree for cancer detection based on microarray data classification. J. Physics: Conf. Ser. 2019, 1192, 012014.
[9] Shukla, A.K.; Tripathi, D. Detecting biomarkers from microarray data using distributed correlation based gene selection. Genes Genom. 2020, 42, 449–465.
[10] Sampathkumar, A.; Rastogi, R.; Arukonda, S.; Shankar, A.; Kautish, S.; Sivaram, M. An efficient hybrid methodology for detection of cancer-causing gene using CSC for micro array data. J. Ambient. Intell. Humaniz. Comput. 2020, 11, 4743–4751.
[11] Kilicarslan, S.; Adem, K.; Celik, M. Diagnosis and classification of cancer using hybrid model based on ReliefF and convolutional neural network. Med. Hypotheses 2020, 137, 109577.
[12] Naser, M.A.; Deen, M.J. Brain tumor segmentation and grading of lower-grade glioma using deep learning in MRI images. Comput. Biol. Med. 2020, 121, 103758.
[13] Lee, J.; Choi, I.Y.; Jun, C.-H. An efficient multivariate feature ranking method for gene selection in high-dimensional microarray data. Expert Syst. Appl. 2021, 166, 113971.
[14] Sukumaran, A., & Abraham, A. (2022). Automated Detection and Classification of Meningioma Tumor from MR Images Using Sea Lion Optimization and Deep Learning Models. *Axioms*, *11*(1), 15.
[15] Karayegen, G., &Aksahin, M. F. (2021). Brain tumor prediction on MR images with semantic segmentation by using deep learning network and 3D imaging of tumor region. *Biomedical Signal Processing and Control*, *66*, 102458.
[16] Krishna, N., Khalander, M. R., Shetty, N., &BharathBhushan, S. N. (2021). Segmentation and detection of glioma using deep learning. In *Advances in Artificial Intelligence and Data Engineering* (pp. 109-120). Springer, Singapore.
[17] Díaz-Pernas, F. J., Martínez-Zarzuela, M., Antón-Rodríguez, M., & González-Ortega, D. (2021, February). A deep learning approach for brain tumor classification and segmentation using a multiscale convolutional neural network. In *Healthcare* (Vol. 9, No. 2, p. 153). Multidisciplinary Digital Publishing Institute.
[18] Gurunathan, A., & Krishnan, B. (2021). Detection and diagnosis of brain tumors using deep learning convolutional neural networks. *International Journal of Imaging Systems and Technology*, *31*(3), 1174-1184.